

Understanding the Habit Modification of Ammonium Dihydrogen Phosphate by Chromium Ions Using a Dopant-Induced Charge Compensation Model

D. A. H. Cunningham

Osaka National Research Institute, Midorigaoka 1-8-31, Ikeda 563, Japan

R. B. Hammond, X. Lai, and K. J. Roberts*[†]

Department of Pure and Applied Chemistry, University of Strathclyde, Glasgow G1 1XL, UK

Received April 14, 1994. Revised Manuscript Received June 19, 1995[©]

The habit modification of ammonium dihydrogen phosphate when grown from an aqueous solution containing $\text{CrCl}_3 \cdot 6\text{H}_2\text{O}$ has been studied using UV-vis spectroscopy and X-ray absorption spectroscopy. Upon incorporation into the crystal lattice, the cationic Cr complex manifests a compression of the bonding distance to the surrounding H_2O shell. The results are rationalized in terms of an incorporation model which replaces a single phosphate ion by a $\text{CrCl}_2(\text{H}_2\text{O})_4^+$ complex. It is proposed that formal charge compensation is obtained through the removal of two hydrogen-bonding protons, from adjacent phosphate groups, and two adjacent ammonium cations.

Introduction

The process of crystallization represents an important separation and purification technique for the chemical industry. In the processing of many speciality materials, consideration of product stability often precludes the use of any other separation technique, such as distillation. Furthermore, crystallization is one of the most energy-efficient industrial processes. In industrial crystallization, optimizing, and controlling crystal morphology is of fundamental importance. An incorrectly defined crystal morphology may have an impact upon a number of important technological areas such as compaction, storage, and filterability. When the crystallization results in an undesirable crystal morphology, habit-modifying additives are often used to control the relative growth rates of the various crystal surfaces of the material in order to optimize a desired particle shape. Such heterogeneous additives are presumed to affect the growth rate of individual crystal faces, either by blocking the movement of step/kink sites or by incorporating in the solid state and disrupting the solid-state bonding networks. However, very few systems have, as yet, been fully studied, and much concerning the physical processes associated with such habit modifying agents remain completely unknown at this time.

The selection and definition of habit modifying additives, which in ionic systems often take the form of trace metallic ions, require the application of structural techniques to assess the nature of the bonding of the ionic additive to the host system. In process technology research ammonium dihydrogen phosphate ($\text{NH}_4\text{H}_2\text{PO}_4$, ADP) has often been used as a representative model system for defining the physical mechanisms that underpin particle formation processes in industrial crystallization systems. This is because ADP grows

comparatively easily, exhibits a well-defined crystal morphology, and has been studied extensively in terms of understanding its growth kinetics. In addition, ADP is well-known^{1–8} to be a useful demonstration system for studying the effects of habit modification by ionic species. However, in respect of the latter, there has been a lack of agreement in defining the structural chemistry associated with the incorporation of the impurity species. In particular, there is a pressing need to develop a consistent model which adequately explains both the site occupied by the impurity and the mechanism by which charge is balanced following incorporation. Thus, even though from experimental work we know which ions typically have the greatest effect on the crystal habit (see, e.g., the work of Kolb and Comer⁷), no serious consideration has been given as to why only certain trivalent transition-metal ions are able to modify the morphology of the ADP host.

Previous work on the habit modification of ADP has suggested that the impurity is incorporated either interstitially^{2–6,8} or at one of the ammonium sites.⁹ The remaining charge imbalance, if any, is then regarded as a simple problem of removing additional ammonium or hydrogen ions, until charge neutrality is achieved. However, neither the previous work nor the literature in general addresses the issue of the mechanism involved. For this, not only should the impurity be able to remove precisely the correct number of counterions,

(1) Jaffe, H.; Kjellgren, B. R. F. *Faraday Discuss. Cryst. Growth* **1951**, *5*, 319.

(2) Davey, R. J.; Mullin, J. W. *J. Cryst. Growth* **1974**, *23*, 89.

(3) Davey, R. J.; Mullin, J. W. *J. Cryst. Growth* **1974**, *26*, 45.

(4) Davey, R. J.; Mullin, J. W. *Kristall. Techn.* **1976**, *11* (3), 229.

(5) Fontcuberta, J.; Rodriguez, R.; Tejada, J. *J. Cryst. Growth* **1978**, *44*, 593.

(6) Mullin, J. W.; Amatavivadhana, A.; Chakraborty, M. *J. Appl. Chem.* **1970**, *20*, 153.

(7) Kolb, H. J.; Comer, J. J. *Am. Chem. Soc.* **1945**, *67*, 894.

(8) Barrett, N.; Lamble, G. M.; Roberts, K. J.; Sherwood, J. N.; Greaves, G. N.; Davey, R. J.; Oldman, R. J.; Jones, D. *J. Cryst. Growth* **1989**, *94*, 689.

(9) Byteva, I. M. *Growth Cryst.* **1968**, *58*, 26.

* Communicating author.

[†] Also at CLRC Daresbury Laboratory, Warrington WA4 4AD, UK.

[©] Abstract published in *Advance ACS Abstracts*, August 1, 1995.

but the process overall should be energetically favorable.

In a recent study on Cu^{2+} -doped ammonium sulfate we proposed a model that not only accounts for the difference in adsorption behavior between differing species but also that was able to rationalize the problem of charge compensation.¹⁰⁻¹² In this work it was found that control of adsorption depends upon the ability of complexed species, in that case water molecules, to mimic the features of the host material. The probability of adsorption is determined by the differences in the oxidation state of the ion used and the number of mimic (or deception) type ligands bound to the central atom. For ammonium sulfate the water molecules attached to the Cu^{2+} ion differ from free unbound water molecules due to the withdrawal of electron density from the oxygen atomic site. This, in turn, causes a charge redistribution within the water molecules until the charge on the hydrogen atoms closely resembles that on the NH_4^+ .¹⁰ This enables the tetrahydrate copper complex to insert itself into the crystal lattice by using the water ligands to mimic the host ammonium ions. With the divalent copper ion replacing the SO_4^{2-} ion, charge imbalance is then easily explained by the removal of four ammonium ions on a one-for-one basis with each of the four water ligands attached to the copper atom. Hence, this explains not only the charge compensation mechanism but also the space required for such a large species and is independent of the transition-metal ion used.

In this paper we now attempt to extend this model and consider its applicability in improving our understanding of the habit modification of ADP by Cr^{III} . $\text{Cl}_3 \cdot 6\text{H}_2\text{O}$. In general this octahedrally coordinated impurity may exist in three distinct isomers which can be easily identified by their color: $\text{Cr}^{\text{III}}(\text{H}_2\text{O})_6\text{Cl}_3$ is violet and has three chlorine ions observable by titration; $[\text{Cr}^{\text{III}}\text{Cl}(\text{H}_2\text{O})_5]\text{Cl}_2 \cdot 2\text{H}_2\text{O}$ is pale green and contains two free chlorines; *trans*- $[\text{Cr}^{\text{III}}\text{Cl}_2(\text{H}_2\text{O})_4]\text{Cl} \cdot 2\text{H}_2\text{O}$ is dark green and has a single free chlorine. In our work only the latter was used. We have employed X-ray absorption spectroscopy and UV-vis spectroscopy in this study to determine the local structure around the incorporation site and have attempted to rationalize the results from these techniques using molecular and crystal modeling techniques.

Experimental Section

Crystal Growth. Crystals (typically $20 \times 5 \times 5 \text{ mm}^3$ in size) of ADP doped with the $[\text{Cr}^{\text{III}}\text{Cl}_2(\text{H}_2\text{O})_4]\text{Cl} \cdot 2\text{H}_2\text{O}$ impurity were prepared by seeded growth from a stirred aqueous solution by the controlled evaporation of solvent at a constant temperature of 35°C .¹² The rate of evaporation of solvent was typically $0.5 \text{ cm}^3/\text{day}$ allowing approximately 0.001 g of material to crystallize each hour. The impurity concentration in the aqueous phase was $2500 \mu\text{g g}^{-1}$, calculated on a metal ion/ADP basis. The concentration in the as grown crystal was not determined.

UV-Vis Spectroscopy. UV-vis spectra of the dopant material, the doped solution, and the resultant doped ADP

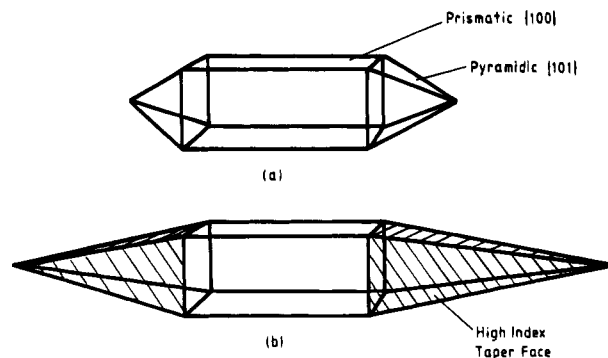


Figure 1. Schematic showing the crystal growth morphology of ADP: (a) pure crystal and (b) crystal doped with $\text{Cr}^{\text{III}}\text{Cl}_2 \cdot (\text{H}_2\text{O})_4^+$ ions. Note the shaded area marked in (b) shows the regions where the dopant is incorporated.

crystal were obtained in transmission mode using a standard UV-vis spectrometer. Spectra from each region of the crystal were obtained by cutting the crystal and analyzing the tapered and prismatic faces separately. Following background subtraction of the data the normalized UV-vis spectra were directly compared.

X-ray Absorption Spectroscopy. X-ray absorption spectra at the Cr K-edge (5889 eV) using fluorescence mode detection were taken on beam line 8.1 at the Daresbury synchrotron radiation source. From these, the extended absorption fine structure (EXAFS) was used to obtain the local atomic structure around the impurity ion (see, for example, Koningsberger and Prins¹³). Full details of the experimental arrangement and data analysis are discussed elsewhere.¹⁰⁻¹² The EXAFS data was analyzed to a radial distance with respect to the Cr atom of ca. 3 \AA .

Molecular Modeling. The modeling package CERIUSt² 14 together with the universal force field^{15,16} was used to calculate the potential energy of the complex relative to the environment of the ADP crystal. Energy minimization was employed to optimize the conformation of the complex in the ADP crystal environment. In this procedure the potential energy of an arbitrary geometry is calculated as the sum of various two-body, three-body, and four-body interactions. The total potential energy is expressed as a sum of valence or bonded interactions and nonbonded interactions.

Results and Discussion

Crystal Growth. The typical growth morphology of ADP is summarized in Figure 1 with the crystal morphology of the undoped crystal (a) dominated by large $\{100\}$ prismatic faces which are capped by much smaller $\{101\}$ faces. The doped crystals (b) differed from the pure sample by the presence of an elongation or tapering of the original $\{101\}$ faces. Visual inspection revealed the characteristic hourglass effect,¹⁷ with the impurities clearly segregated to the capping regions of the crystal. The capped regions exhibited the characteristic green coloration of the $[\text{Cr}^{\text{III}}\text{Cl}_2(\text{H}_2\text{O})_4]\text{Cl} \cdot 2\text{H}_2\text{O}$ complex.

UV-Vis Spectroscopy. Figure 2 shows the UV-vis spectra for the $\text{Cr}^{\text{III}}\text{Cl}_2(\text{H}_2\text{O})_4^+$ ion in (a) its native $[\text{Cr}^{\text{III}}\text{Cl}_2(\text{H}_2\text{O})_4]\text{Cl} \cdot 2\text{H}_2\text{O}$ crystalline state, (b) the saturated doped aqueous solution, and (c) the doped colored

(10) Cunningham, D. A. H.; Armstrong, D. R.; Clydesdale, G.; Roberts, K. J. *J. Chem. Soc., Faraday Discuss.* **1993**, *95*, 347.

(11) Armstrong, D. R.; Cunningham, D. A. H.; Roberts, K. J.; Sherwood, J. N. In *X-Ray Absorption Fine Structure*; Hasnain, S., Ed.; Ellis Horwood: Chichester, 1991; p 435.

(12) Cunningham, D. A. H. *Synchrotron Radiation Studies of Structural Aspects of Crystal Growth*, Ph.D. Thesis, University of Strathclyde, Glasgow, UK, 1991.

(13) Koningsberger, D. E.; Prins, R. *X-ray Absorption: Principles, Applications and Techniques of EXAFS, SEXAFS and XANES*; Wiley: New York, 1988.

(14) Cerius², Computational instruments for materials research, Molecular Simulations International, Cambridge, UK.

(15) Rappe, A. K.; etc. *J. Am. Chem. Soc.* **1992**, *114*, 10024.

(16) Rappe, A. K.; etc. *J. Am. Chem. Soc.* **1992**, *114*, 10046.

(17) Buckley, H. E. *Crystal Growth*; Wiley: New York, 1951.

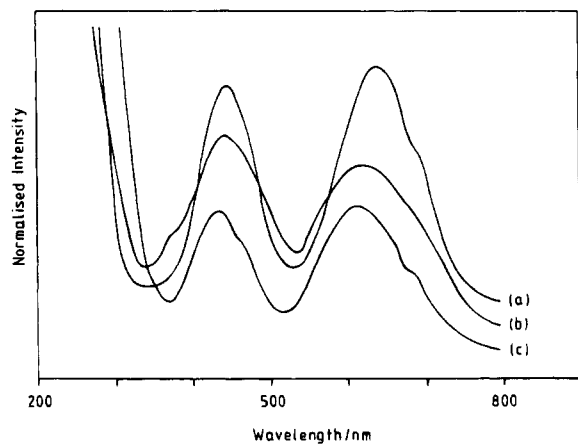


Figure 2. UV-vis spectra taken of: (a) crystalline $[\text{Cr}^{\text{III}}\text{Cl}_2(\text{H}_2\text{O})_4]\text{Cl}\cdot 2\text{H}_2\text{O}$; (b) ADP in saturated aqueous solution containing $2500 \mu\text{g g}^{-1}$ (metal ion/ADP) of $[\text{Cr}^{\text{III}}\text{Cl}_2(\text{H}_2\text{O})_4]\text{Cl}\cdot 2\text{H}_2\text{O}$; (c) the tapered coloured regions of an ADP single crystal grown from saturated ADP solution containing $2500 \mu\text{g g}^{-1}$ (metal ion/ADP) $[\text{Cr}^{\text{III}}\text{Cl}_2(\text{H}_2\text{O})_4]\text{Cl}\cdot 2\text{H}_2\text{O}$. The intensity of absorption signal is normalized for ease of comparison.

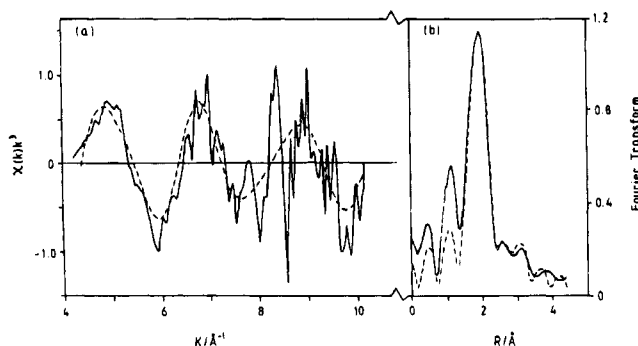


Figure 3. X-ray absorption spectroscopy results showing the theoretical fit (---) to the experimental (—) data: (a) EXAFS; (b) Fourier transform. Data were taken in fluorescence mode at the Cr K-edge (5889 eV) from the tapered colored regions of a single crystal of ADP grown from a saturated ADP solution containing $2500 \mu\text{g g}^{-1}$ (metal ion/ADP) of $[\text{Cr}^{\text{III}}\text{Cl}_2(\text{H}_2\text{O})_4]\text{Cl}\cdot 2\text{H}_2\text{O}$.

region of the crystal. The observed spectra for the dopant compound is consistent with a trivalent Cr(III) ionic state and agrees well with previous work.¹⁸ However, the initial peak in the spectra, at 445 nm, is some 10 nm red shifted compared with the ADP-doped crystal. From crystal field theory such shifts can be accounted for by changes in the energy separation between axial and nonaxial orbitals in MX_2Y_4 complexes. Therefore, as the wavelength decreases the energy separation between the axial and nonaxial orbitals increases. As the general shape and position of the three spectra are similar, this suggests that upon absorption, the impurity remains more or less unperturbed. The slight differences in wavelength may therefore result from the presence of strain within the impurity, caused by compression along one or more of the bonds. As with the visual examination, no evidence for Cr^{3+} segregation outside the coloured capping regions could be detected using UV-vis spectroscopy.

X-ray Absorption Spectroscopy. Figure 3 and Table 1 show the EXAFS data taken from the doped crystal together with the fitted structural parameters.

Table 1. Results from the Fitting of the EXAFS Data Taken of the Tapered Colored Regions of a Single Crystal of ADP Grown from a Saturated ADP Solution Containing $2500 \mu\text{g g}^{-1}$ (Metal Ion/ADP) of $[\text{Cr}^{\text{III}}\text{Cl}_2(\text{H}_2\text{O})_4]\text{Cl}\cdot 2\text{H}_2\text{O}$ (Standard Deviations in Parentheses^a)

atom type	coordination no.	distance/Å	Debye-Waller factor/Å ²
EXAFS			
O	3.0 (0.53)	1.97 (0.02)	0.004 (0.001)
Cl	0.9 (0.38)	2.33 (0.06)	0.011 (0.004)
N or O	4.0 (0.48)	2.91 (0.04)	0.023 (0.010)
Literature (Morosin ¹⁶)			
O	4	2.002–2.013	
Cl	2	2.286	

^a For the purposes of comparison, the literature¹⁶ values for the bulk phase of $[\text{Cr}^{\text{III}}\text{Cl}_2(\text{H}_2\text{O})_4]\text{Cl}\cdot 2\text{H}_2\text{O}$ are also given.

Table 2. Predicted Charge Imbalance Generated by Placing Each Isomer Substitutionally at the Phosphate Site, with the Effective Charge Compensation upon Replacing Ammonium Ions by Water Ligands on a One-for-One Basis^a

complex	charge imbalance	no. of H ₂ O ligands	net charge	ref
$\text{Cr}(\text{H}_2\text{O})_6^{3+}$	+6	6	0	this work
$\text{CrCl}(\text{H}_2\text{O})_5^{2+}$	+5	5	0	this work
$\text{CrCl}_2(\text{H}_2\text{O})_4^+$	+4	4	0	this work
$\text{Fe}(\text{H}_2\text{O})_6^{3+}$	+6	6	0	6
$[\text{Fe}(\text{H}_2\text{O})_5(\text{OH})]^{2+}$	+5	5	0	6
$[\text{Fe}(\text{H}_2\text{O})_4(\text{OH})_2]^+$	+4	4	0	6
$\text{Fe}(\text{H}_2\text{O})_6^{2+}$	+5	6	-1	6
$\text{M}(\text{H}_2\text{O})_4^{2+}$	+5	4	+1	7
$\text{M}(\text{H}_2\text{O})_6^{2+}$	+5	6	-1	6

^a Also shown is the predicted charge imbalance for a variety of Fe^{3+} and Fe^{2+} ions along with those predicted for general M^{2+} ions present as hydrated species. Note that standard aqueous chemistry is assumed in which the effect of chlorine ions has been ignored.

As with UV-vis spectroscopy no dopant species could be detected outside the capping regions. From the literature the trivalent chromium ion is known¹⁹ to occupy a distorted octahedral environment in which the water molecules and chlorine atoms may be divided into two distinct shells. The first shell is a distorted square composed of four water molecules, in a two-plus-two arrangement lying at distances of between 2.002 and 2.013 Å from the Cr atom. The second shell at 2.286 Å contains the chlorine species.

From the EXAFS data we could identify three shells associated with different species. The first of these at 1.97 Å belongs to oxygen atoms which we presume to be associated with water molecules (as confirmed by UV spectroscopy), the second at 2.33 Å belongs to chlorine atoms and the third, lying at 2.91 Å belongs to an unidentified atomic species consistent with either nitrogen or oxygen atoms. These latter atoms, due to the similarity of their backscattering amplitudes, cannot easily be discriminated by EXAFS. We found no evidence for the elongated Cr–O correlation of 2.013 Å, associated with the binding of water molecules, as indicated by Morosin¹⁹ (see Table 1). Thus, these results indicate that upon entering the ADP lattice there is a compression or contraction of the second water shell distance with respect to the bulk crystal structure of $[\text{Cr}^{\text{III}}\text{Cl}_2(\text{H}_2\text{O})_4]\text{Cl}\cdot 2\text{H}_2\text{O}$.¹⁶ The overall occupancy numbers are slightly lower than those found in literature

(18) Elving, P. J.; Zemel, B. *J. Am. Chem. Soc.* **1957**, *79*, 1281.

(19) Morosin, B. *Acta Crystallogr.* **1966**, *21*, 280.

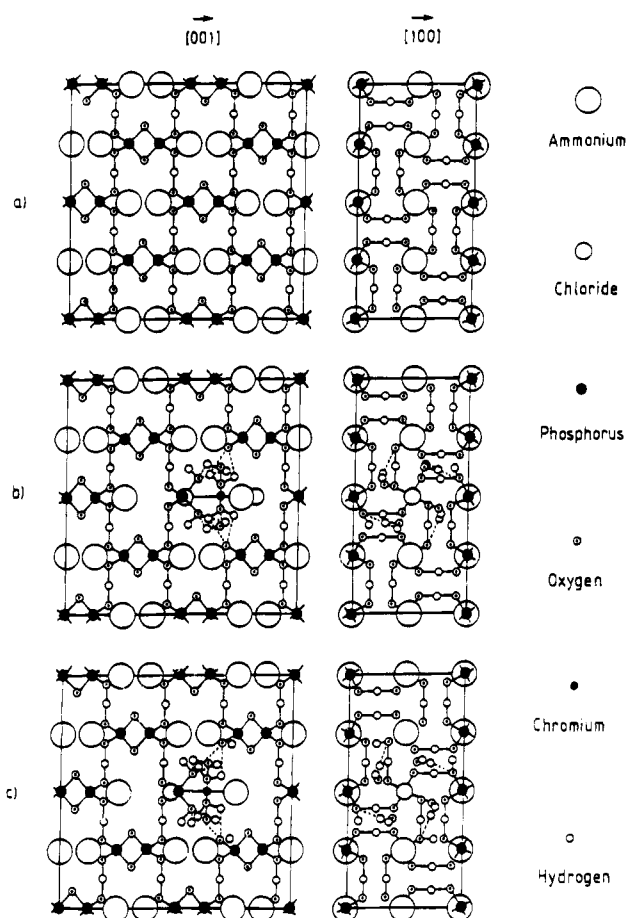


Figure 4. Pure and $\text{CrCl}_2(\text{H}_2\text{O})_4^+$ -doped ADP crystal lattice projections. (a) Pure ADP lattice projections of (010) and (001). (b) Doped ADP lattice projections of (010) and (001) by moving the complex 0.47 Å along the (001) axis. (c) Doped ADP projections of (010) and (001), the complex remains centred on the phosphorus atom site and two protons are disordered between the four adjacent phosphate groups. For clarity of presentation the ammonium cations are given as spheres.

but are within acceptable limits of error (typically $\pm 20\%$) for this technique.

Charge Compensation. From a chemical standpoint the adsorption of the Cr^{3+} impurity ionic complex without significant modification of the structural chemistry is not surprising. The Cr^{3+} ion is well-known for its high chemical stability and within the aqueous solution is likely to react only over long time periods. Table 2 lists the predicted charge imbalance assuming that the impurity occupies a phosphate anionic site, the number of water ligands attached to the impurity and the predicted net charge upon the crystal if each water ligand can replace either one ammonium ion or a dihydrogen proton. Also included for comparison purposes are details of some of the transition metal ions examined by Mullin et al.⁶ and by Kolb and Comer.⁷ From a simple comparison of each of the transition-metal ions, a surprisingly good correlation is found between the impurities which are adsorbed, and a charge imbalance equal to the number of water ligands, in accordance with our model. In this model, providing each transition metal is octahedrally coordinated and exists as a stable isomer, only those complexes which have an equivalent number of water ligands to the charge differential between the impurity and phosphate can be incorporated into the crystal. Hydrated **divalent**

Table 3. Bond Lengths within the Complex and the Distances between Complex Atoms and Surrounding Atoms, after Relaxing the Positions of the 8 H Atoms Associated with the Water Ligands and Allowing Translation of the Whole Complex along the Crystallographic *c* Axis

type of the bonds (or distances)	between atoms	length/Å
distances within the complex	H-O	0.988
	Cr-O	1.970
	Cr-Cl	2.330
	Cl1-H1	2.710
	Cl2-H2	2.826
	Cl1-H3	3.118
hydrogen bonds	Cl2-H4	2.639
	H1-O	2.127
	H2-O	2.200
	H3-O	2.483
closest distances between the complex and the surrounding atoms	H4-O	2.337
	O-O	2.48
	H-H	2.230

ions belonging to the octahedral class are thus likely to be rejected and can be expected to have no effect on the growth process. Using this approach we are therefore able to predict that all three of the $\text{Cr}^{\text{III}}\text{Cl}_3\cdot 6\text{H}_2\text{O}$ isomers as well as most other trivalent ions should, in principle, be able to exist as stable species within the ADP crystal lattice. Whilst it should be noted that we have not been able to locate any previous work relating to $\text{Cr}^{\text{III}}\text{Cl}(\text{H}_2\text{O})_5^{2+}$ and $\text{Cr}(\text{III})(\text{H}_2\text{O})_6^{3+}$, in each case where a system has been successfully studied, each of the experimental observations fit well within this overall scheme.

Structural Model. Under ambient conditions ADP crystallizes with four molecules in a tetragonal unit cell (space group $I\bar{4}2d$).²⁰ The crystal chemistry is dominated by anionic phosphate groups (centered at 0.0, 0.0, 0.0 and 0.5, 0.0, 0.25) bonded together by a 3-d network of hydrogen bonds. To maintain the tetragonal symmetry the dihydrogen proton sites adjacent to each phosphate oxygen are 50% disordered along the O-H...O bond axes. Within this rigid framework the ammonium cations (centered at 0.0, 0.0, 0.5 and 0.5, 0.0, 0.75) fit between the closely packed phosphate groups of the structure (e.g., see Figure 4a).

Given the size of the octahedral complex $\text{Cr}^{\text{III}}\text{Cl}_2(\text{H}_2\text{O})_4^+$, the tetrahedral environment of the phosphate anion, and the rigid hydrogen-bonding network of the ADP crystal structure, it is unlikely that a simple ionic substitution model involving the creation of Schottky or Frenkel defects (as expected for simple AB_n -type atomic solids) will apply here. Previous studies have suggested that the additive $\text{CrCl}_2(\text{H}_2\text{O})_4^+$ is incorporated either at interstitial sites^{2-6,8} or at ammonium sites⁹ of ADP. In this work, the interstitial and ammonium sites were carefully examined using molecular modeling methods.¹⁴ It was concluded that these sites are too small to accommodate the impurity complex, its size having been determined by previous work^{19,21,22} and specified by the EXAFS analysis above. Conversely, it was estimated that the phosphate anion site is large enough to accommodate the complex. Intuitively, there appears to be no obvious structural relationship between the complex and proposed host site given their respec-

(20) Tenzer, L.; Frazer, B. C.; Pepinsky, R. *Acta Crystallogr.* **1958**, *11*, 505.

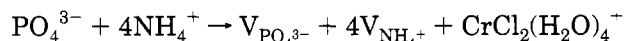
(21) von Schnering, H. G.; Brand, B. H. *Z. Anorg. Allg. Chem.* **1973**, *402*, 159.

(22) Dan, I. G.; Freeman, H. C. *Inorg. Chem.* **1965**, *4*, 1555.

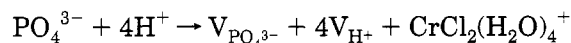
tive octahedral and tetrahedral symmetries. However, it was decided to postulate a structural model based on ion replacement at the phosphate anion site, and to test this by applying molecular modeling techniques.

Maintaining a charge balance of the formal point charges demands the formation of either cationic or anionic vacancies (V_{site}). There are three possibilities:

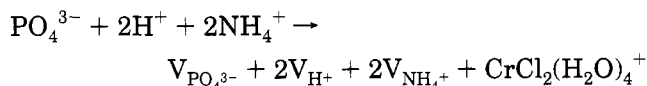
The impurity complex could displace a phosphate anion and four ammonium cations (a):



The impurity complex could displace a phosphate anion and four protons (b):



The impurity complex could displace a mixed group of ammonium ions and protons (c):



With case (a), the four NH_4^+ cations adjacent to a phosphate site define too large a volume compared to the complex, so it may be discounted. Cases (b) and (c) are now considered in more detail.

Both the $\text{CrCl}_2(\text{H}_2\text{O})_4^+$ cation and phosphate anion have 4-fold symmetry axes, (rotation and inversion, respectively), these lie along the Cl–Cr–Cl direction in the complex and the c axis in the ADP crystal. Therefore, in our initial model, upon substituting the complex for a phosphate anion, the Cl–Cr–Cl direction was aligned with the c axis of the crystal and the chromium cation centered on the phosphorus position. Considering nonbonded contacts between atoms, it was found that the two adjacent NH_4^+ cations along the c axis could not be accommodated given this orientation of the complex, hence case (b) was eliminated.

Having, therefore, concluded that case (c) applies here, two alternative idealized models for the incorporation of the complex were examined by calculating the potential energy of the complex with respect to the ADP environment.

(i) The complex is disordered between two positions defined by an equal but opposite displacement of the central chromium cation, from the phosphorus atom site, along the c -axis direction (i.e., from (0,0,0) to (0,0, ± 0.125) etc.). Hence the chromium cation is 50% disordered between these two sites. At the same time, two protons are associated with the pair of adjacent phosphate anions which have two oxygen atoms centered on the plane opposite to the chromium cation.

(ii) The complex remains centered on the phosphorus atom site and two protons are disordered between the four adjacent phosphate groups.

Keeping the main octahedral frame of $\text{CrCl}_2(\text{H}_2\text{O})_4^+$ rigid and allowing only the eight hydrogen atoms of the water ligands to relax, the potential energy of the complex as a whole was evaluated for the two models outlined above. In the second model, it was envisaged that the hydrogen atoms of the water ligands in the complex could form hydrogen bonds, with the four surrounding phosphate anions, in an arrangement mimicking the hydrogen bonding in the unperturbed structure (e.g., see Figure 4c). In fact, the minimum

Table 4. Fractional Coordinates for the Atoms in the Chromium Complex and the Two Disordered Protons Resulting from the Molecular Modeling Calculations^a

	x/a	y/a	z/c
Cr	0.000	0.000	0.068
Cl1	0.000	0.000	0.378
Cl2	0.000	0.000	-0.242
O1	0.105	-0.241	0.068
O2	0.241	0.105	0.068
O3	-0.105	0.241	0.068
O4	-0.241	-0.105	0.068
H1	0.162	0.243	0.184
H2	0.192	-0.249	-0.031
H3	0.222	0.222	0.112
H4	0.274	0.118	-0.054
H5	-0.162	0.257	0.184
H6	-0.192	0.249	-0.033
H7	-0.222	-0.222	0.112
H8	-0.274	-0.118	-0.044
H _a	-0.238	-0.370	-0.207
H _b	0.238	0.370	-0.207

^a These are given with respect to the fractional coordinates for the ADP given from the crystal structure.

Table 5. Bond Lengths within the Complex and the Distances between the Complex Atoms and Surrounding Atoms When the Complex Remains Centered on the Phosphorus Atom Site and Two Protons Are Disordered between the Four Adjacent Phosphate Groups

type of bonds (or distances)	between atoms	length/Å
distances within the complex	H–O	0.982
	Cr–O	1.970
	Cr–Cl	2.330
	Cl1–H1	2.649
	Cl1–H2	2.748
hydrogen bonds	H–O	2.250
	O–O	2.620
closest distances between the complex and the surrounding atoms	H1–H _a	2.100
	H2–H _b	2.575

potential energy was obtained on displacement of the central chromium cation 0.47 Å along the [001] axis from the phosphorous atom site (e.g., see Figure 4b). This positioning of the complex corresponds to its location at (0,0, ± 0.063) and represents an average of the orientations in the two idealized models. For this orientation the bond lengths within the complex and the distances between atoms of complex and the surroundings are listed in Table 3. The coordinates of the complex in a single unit cell are summarized in Table 4. Since the difference in potential energy relative to placing the complex on the phosphorus atom site (second model) is small, the bond lengths within the complex, and the distances between atoms of complex and the surroundings are also summarized for this position (Table 5) along with the fractional coordinates of the complex in a single unit cell (Table 6).

As a footnote to this discussion, it should be noted that there is the possibility that the third (weakly bound) chlorine atom associated with the dopant may be involved in the habit modification process. Davey and Mullin² reported a 1:1 ratio of free chlorine to chromium. As their titration method was insensitive to the strongly bound inner shell chlorine atoms in the $\text{Cr}^{\text{III}}\text{Cl}_2(\text{H}_2\text{O})_4^+$ complex, this may have resulted in their incorrect identification of the incorporated impurity as a simple hydrate. This may also explain the discrepancies between their work and the Mössbauer studies of Fontcuberta et al.⁵ From our work the role of the third chlorine atom is not clear. However, previous

Table 6. Fractional Coordinates for the Atoms in the Chromium Complex and Protons Disordered between the Four Phosphate Groups Resulting from the Molecular Modeling Calculations^a

	<i>x/a</i>	<i>y/z</i>	<i>z/c</i>
Cr	0.000	0.000	0.000
Cl	0.000	0.000	0.308
Cl	0.000	0.000	-0.308
O1	0.106	-0.241	0.000
O2	0.241	0.106	0.000
O3	-0.106	0.241	0.000
O4	-0.241	-0.106	0.000
H1	0.141	-0.263	0.120
H2	0.213	-0.234	-0.077
H3	0.234	0.213	0.078
H4	0.263	0.141	-0.120
H5	-0.106	0.263	0.120
H6	-0.213	0.234	-0.077
H7	-0.234	-0.213	0.078
H8	-0.263	-0.141	-0.120
Ha	0.417	-0.254	0.202
Hb	0.254	0.417	-0.202
Hc	-0.417	0.254	0.202
Hd	-0.254	-0.417	-0.202

^a These are given with respect to the fractional coordinates for the ADP given from the crystal structure.

work has shown chlorine to have no significant effect on the growth process,⁷ it is likely that the weakly bound chlorine, if incorporated by ADP, occupies separate sites

from the $\text{Cr}^{\text{III}}\text{Cl}_2(\text{H}_2\text{O})_4^+$ complex. Further work is clearly needed to quantify this.

Conclusions

UV-vis and X-ray absorption spectroscopy studies of the habit modification of ADP when crystallized in presence of trace chromium ions are consistent with the adsorption of a tetraaquodichloro complex of the chromium ion during growth. The adsorption of the complex ion can be rationalised by a simple charge compensation model. In this the charge imbalance created by the adsorption of a *trans*- $\text{Cr}^{\text{III}}\text{Cl}_2(\text{H}_2\text{O})_4^+$ impurity complex which replaces a phosphate anion, is offset by removal of two adjacent ammonium ions and two dihydrogen protons from two adjacent phosphate groups. The data are thus in agreement with our previous work on doped ammonium sulphate¹⁰⁻¹² and suggests that this model may be transferable to other systems.

Acknowledgment. This work was supported by SERC Grant GR/F/49323. We gratefully acknowledge Daresbury Laboratory for the provision of synchrotron radiation beam time and to one of the referees for directing us to ref 16.

CM940192V